Photophysical Properties of New Psoralen Derivatives: Psoralens Linked to Adenine through Polymethylene Chains§

Dong Jin Yoo,* Hyung-Du Park, Ae Rhan Kim,* Young S. Rho,† and Sang Chul Shim‡

Department of Chemistry, Seonam University, Namwon 590-711, Korea
†Department of Chemistry, Chonbuk National University, Chonju 561-756, Korea
‡Center for Molecular Design and Synthesis, Department of Chemistry and School of Molecular Science-BK21, Korea Advanced Institute of Science and Technology, Daejeon 305-701, Korea
Received March 27, 2002

The model compounds, 8-methoxypsoralen-$CH_2O(CH_2)_n$-adenine (MOPCH$_2$OCnAd, n=2, 3, 5, 6, 8, and 10) in which 5 position of 8-methoxypsoralen (8-MOP) is linked by various lengths of polymethylene bridge to N^9 of adenine. UV absorption spectra are identical with the sum of MOPCH$_2$OC3 and adenine absorption spectra. Solvent effects on the UV absorption and fluorescence emission spectra indicate that the lowest excited singlet state is the ($\pi\rightarrow\pi^*$) state. The spectral characteristics of the fluorescence of MOPCH$_2$OCnAd are strongly dependent upon the nature of the solvents. The fluorescence emission spectra in aprotic solvents are broad and structureless due to the excimer formation through the folded conformation accelerated by hydrophobic π-π stacking interaction. Increasing polarity of the protic solvents leads to higher population of unfolded conformation stabilized through favorable solvation and H-bonding, and consequently to an increase in the fluorescence intensity, fluorescence lifetime, and a shift of fluorescence maximum to longer wavelengths. The decay characteristics of the fluorescence in polar protic solvents shows two exponential decays with the lifetimes of 0.6-0.8 and 1.6-1.9 ns in 5% ethanol/water, while MOPCH$_2$OC3 shows 0.5 and 1.7 ns fluorescence lifetimes. The long-lived component of fluorescence can be attributed to the relaxed species (*i.e.*, the species for which the solvent reorientation (or relaxation) has occurred), while the short-lived components can be associated with the unrelaxed, or only partially relaxed, species.

Key Words : Psoralen derivatives, UV spectra, Fluorescence spectra, Time-resolved fluorescence emission decay, Solvent effects

Introduction

The ability of psoralens to complex with DNA in the ground state by intercalation has been well established[1] and many psoralens are employed as the photosensitizing agents for the treatment of various skin diseases,[2-5] *e.g.*, psoriasis, vitiligo, mycosis fungoides, chromic leukemia, and some infections connected with AIDS.[6] In addition to medicinal applications, psoralens have been used as molecular probes in elucidating the structure of many important biological macromolecules.[7,8] A large number of studies on the mechanism of the photochemical reactions between psoralen and DNA bases *in vivo*[1,9] or with thymine derivatives[10,11] have been carried out. These studies involved intermolecular processes leading generally to a mixture of several photoproducts. Binding of psoralens to DNA is generally the consequence of two successive events: (a) intercalation of the psoralen between the base pairs of nucleic acids in the ground state.[12,13] (b) [2+2] type photoconjugation of the 3,4-pyrone and/or 4',5'-furan double bond of complexed psoralen to pyrimidine 5,6 double bond.[9,14] The formation of the intercalated complex between psoralens and DNA is an important step which markedly affects the successive covalent photobinding to the macromolecule.[12,13] To investigate these two processes in the absence of complicating factors associated with hydrogen bonding or the usual carbohydrate and phosphodiester linkages, Lhomme and Decout[15] prepared a series of model compounds **4** starting from 8-hydroxypsoralen (**2**) and showed that the polymethylene bridges allow intramolecular ring-ring stacking of the two chromophores in the molecules. Castellan *et al.*[16] also investigated the interactions and the photoreactions of synthetic psoralens containing psoralen and thymine rings, two psoralen rings (**3** and **5**), or two thymine rings. The reactivity of the bispsoralen **5** were reported to be sensitive to the presence of cations because the cations added caused the conformation of the polyoxyethylene chain folded, increasing the intramolecular interaction between two psoralen chromophores. Recently, Shim *et al.* suggested that the photoreaction of psoralen with DNA proceeds by adenosine-mediated electron transfer from/to psoralen to/from thymine base.[17,18] Moreover, they reported that the poly[dA-dT]·poly[dA-dT] sequence region is the most favorable site for the photocycloaddition reactions of furocoumarins.[17] Because of the importance of interaction between the 8-methosypsoralen and purine base pairs in DNA, we prepared some model

§Dedicated to Professor Sang Chul Shim for his distinguished achievements in chemistry and outstanding contributions to the Korea Chemical Society.

*Author to whom correspondence should be addressed. Fax: +82-63-620-0023; e-mail: djyoo@tiger.seonam.ac.kr

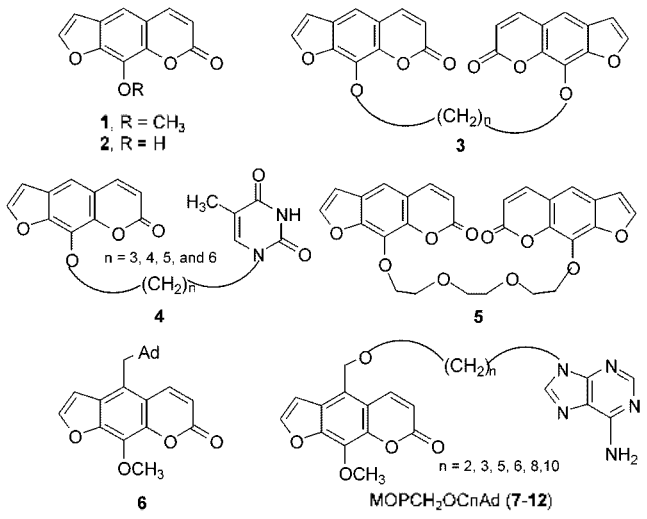

Figure 1. Chemical structures of 8-MOP (**1**), 8-hydroxypsoralen (**2**), psoralen analogues (**3-5**), $MOPCH_2Ad$ (**6**), and $MOPCH_2O$-CnAd (**7-12**).

compounds (**6-12**), the bifunctional psoralen derivatives having an adenine as electron donor linked by a varying length of polymethylene bridges starting from **1**, and studied intramolecular ring-ring stacking interactions between the two aromatic moieties.[19] In this paper, we report some photophysical properties of these compounds including the role of adenine ring in the complexation process.

Materials and Methods

Instruments. The ^{1}H-NMR and ^{13}C-NMR spectra were recorded on Brüker AM-400 MHz spectrometer. Proton chemical shifts (δ) are reported in ppm downfield from tetramethylsilane (TMS), and ^{13}C resonance peak of the solvent as an internal reference and reported in ppm downfield from TMS. Fourier transform infrared spectra (FTIR) were recorded on a Nicolet 5-DXB series FT-IR spectrophotometer. Mass spectra were determined at 70 eV with V.G. AutoSpec Ultima by the electron impact (EI) method. UV absorption spectra were recorded on a Shimadzu 3100S spectrophotometer. Fluorescence spectra were recorded on a Perkin-Elmer LS-50 luminescence spectrometer with a gated photomultiflier tube detector at room temperature. The time-resolved fluorescence decay curve was obtained by time-correlated single photon counting (TCSPC) technique. The excitation source was a cavity-dumped dual-jet picosecond dye laser (Coherent, model 702) synchronously pumped by a mode-locked Ar ion laser (Coherent, Innova 200). Nanosecond Nd : YAG laser (frequency-tripled 355 nm) pulse and Xenon arc lamp was used for the excitation and analytical probe light for laser flash photolysis study. Melting points were determined in capillary tubes on a Thomas Hoover capillary melting point apparatus.

Chemicals. 8-Methoxypsoralen and adenine were purchased from Sigma Chemical Co. or Aldrich Co. and used without further purification. All solvents were reagent grade or HPLC grade and purified according to the literature procedures.[20] Bulk grade hexane was distilled prior to use. Spectroscopic grade acetonitrile (CH_3CN), benzene, chloroform, dimethyl sulfoxide (DMSO), ethanol, methanol, methylene chloride, and tetrahydrofuran (THF) were purchased from Merck and used as received. 8-Methoxypsoralen-$CH_2O(CH_2)_n$-adenine ($MOPCH_2OCnAd$, n = 2, 3, 5, and 6; compound **7**, **8**, **9**, and **10**) were synthesized from 8-methoxypsoralen and adenine.[19] The new compounds, $MOPCH_2Ad$ (**6**), $MOPCH_2OC8Ad$ (**11**) and $MOPCH_2OC10Ad$ (**12**) including intermediates such as $MOPCH_2OCnOH$ and $MOPCH_2OCnBr$ were obtained through one step or three steps by the known procedures.[19] Methods and analytical and spectroscopic data for individual intermediates and target materials were as follows:

Preparation of $MOPCH_2Ad$ (6). 5-Chloromethyl-8-methoxypsoralen (0.31 g, 1.17 mmol) prepared from 8-methoxypsoralen[21] was added to a stirred mixture of adenine (0.19 g, 1.41 mmol), K_2CO_3 (0.39 g, 2.81 mmol), and catalytic amounts of KI (19.0 mg) in DMF (12 mL). The stirring was continued for 48 hr at room temperature. The mixture was filtered and the filter cake was washed with ethyl acetate. Following removal of the solvent *in vacuo*, the residue was chromatographed with 10% methanol/methylene chloride to give $MOPCH_2Ad$ **6** (0.30 g, 71%) as a white solid: mp 263-265 °C; ^{1}H-NMR (400 MHz, DMSO-d_6) δ 4.16 (s, 3H), 5.84 (s, 2H), 6.52 (d, 1H, J = 9.9 Hz), 7.31 (d, 1H, J = 2.2 Hz), 7.54 (bs, 1H), 8.10 (s, 1H), 8.14 (d, 1H, J = 2.2 Hz), 8.23 (s, 1H), 8.71 (d, 1H, J = 9.9 Hz); ^{13}C-NMR (100 MHz, DMSO-d_6) δ 60.95, 105.70, 114.53, 115.00, 118.83, 126.57, 132.11, 140.69, 141.56, 142.92, 146.30, 148.08, 149.05, 151.41, 155.03, 159.15; Mass (m/e) 102, 158, 186, 201, 229, 230, 363; HRMS Calcd for $C_{18}H_{13}N_5O_4$: 363.0968, found: 363.0976.

Preparation of $MOPCH_2OC8OH$. 5-Chloromethyl-8-methoxypsoralen (0.91 g, 3.42 mmol) was mixed with 1,8-octanediol (5.0 g, 34.2 mmol), and heated to 90-100 °C with stirring for 12 hr and cooled to room temperature. The resulting mixture was concentrated and column chromatographed with 50% ethyl acetate/hexane to give $MOPCH_2OC8OH$ (0.35 g, 49%) as white solid: mp 79.5-81.5 °C; ^{1}H-NMR (400 MHz, DMSO-d_6) δ 1.25-1.30 (m, 8H), 1.47-1.57 (m, 4H), 3.45 (t, 2H, J = 6.5 Hz), 3.59 (t, 2H, J = 6.6 Hz), 4.24 (s, 3H), 4.82 (s, 2H), 6.38 (d, 1H, J = 9.9 Hz), 6.91 (d, 1H, J = 2.2 Hz), 7.67 (d, 1H, J = 2.2 Hz), 8.13 (d, 1H, J = 9.9 Hz); ^{13}C-NMR (100 MHz, $CDCl_3$) δ 25.61, 26.04, 29.25, 29.28, 29.61, 32.66, 61.33, 62.88, 66.42, 70.65, 105.42, 114.53, 115.27, 120.69, 126.53, 132.53, 141.23, 143.71, 146.50, 146.91, 160.22; IR (cm^{-1}) 3407, 3116, 2932, 2864, 1729, 1587, 1476, 1420, 1384, 1311, 1136, 1088, 1040, 831, 755; Mass (m/e) 175, 186, 201, 217, 229, 245, 374. HRMS Calcd for $C_{21}H_{26}O_6$: 374.1729, found: 374.1727.

Preparation of $MOPCH_2OC10OH$. Reaction of 5-chloromethyl-8-methoxypsoralen (0.66 g, 2.48 mmol), 1,10-decanediol (8.64 g, 49.6 mmol) in DMF (10 mL) was carried out as described for the preparation of $MOPCH_2OC8OH$ to yield $MOPCH_2OC10OH$ (0.47 g, 47%) as white solid: mp 69-71 °C; ^{1}H-NMR (400 MHz, $CDCl_3$) δ 1.16-1.35 (m,

12H), 1.49-1.57 (m, 5H), 3.45 (t, 2H, J = 6.4 Hz), 3.60 (t, 2H, J = 6.4 Hz), 4.25 (s, 3H), 4.82 (s, 2H), 6.38 (d, 1H, J = 9.9 Hz), 6.91 (d, 1H, J = 2.2 Hz), 7.66 (d, 1H, J = 2.2 Hz), 8.13 (d, 1H, J = 9.9 Hz); ^{13}C-NMR (100 MHz, $CDCl_3$) δ 25.67, 26.10, 29.27, 29.32, 29.43, 29.63, 32.73, 61.31, 62.96, 63.00, 66.44, 70.70, 105.42, 114.53, 115.30, 120.74, 126.51, 132.57, 141.21, 143.21, 143.77, 146.46, 146.96, 160.18; IR (cm^{-1}) 3427, 3116, 2932, 2854, 1729, 1587, 1476, 1423, 1384, 1311, 1132, 1093, 1038, 831, 762; Mass (m/e) 186, 201, 217, 229, 230, 245, 402. HRMS Calcd for $C_{23}H_{30}O_6$: 402.2042, found: 402.2055.

Preparation of MOPCH$_2$OC8Br. To a magnetically stirred solution of MOPCH$_2$OC8OH (0.33 g, 0.88 mmol) and carbon tetrabromide (0.59 g, 1.77 mmol) in methylene chloride (10 mL) was added triphenylphosphine (0.49 g, 1.86 mmol) portionwise with ice-bath cooling. Upon completion of the reaction, ice-water (10 mL) was added and the oily suspension was extracted with methylene chloride (50 mL × 3). The organic extract was dried with magnesium sulfate, and the solvent was removed *in vacuo*. The resulting material was dissolved in ethyl acetate and subjected to column chromatography on silica gel with 30% ethyl acetate/hexane which gave MOPCH$_2$OC8Br (0.31 g, 81%) as white solid: mp 56.5-58 °C. ^{1}H-NMR (400 MHz, $CDCl_3$) δ 1.25-1.36 (m, 4H), 1.55 (q, 2H), 1.79 (q, 2H), 3.35 (t, 2H, J = 6.8 Hz), 3.45 (t, 2H, 6.4 Hz), 4.24 (s, 3H), 4.81 (s, 2H), 6.37 (d, 1H, J = 9.8 Hz), 6.91 (d, 1H, J = 2.2 Hz), 7.66 (d, 1H, J = 2.2 Hz), 8.12 (d, 1H, J = 9.8 Hz); ^{13}C-NMR (100 MHz, $CDCl_3$) δ 26.01, 27.99, 28.59, 29.11, 29.59, 32.66, 33.95, 61.31, 66.43, 70.66, 105.42, 114.53, 115.25, 120.66, 126.51, 132.52, 141.18, 143.70, 146.49, 146.90, 160.15; IR (cm^{-1}) 3075, 2932, 2858, 1723, 1590, 1467, 1430, 1338, 1301, 1129, 1038, 846, 753; Mass (m/e) 186, 201, 217, 229, 436, 438; HRMS Calcd for $C_{21}H_{25}BrO_5$: 436.0885, found: 436.0877.

Preparation of MOPCH$_2$OC10Br. Reaction of MOPCH$_2$OC10OH (0.39 g, 0.98 mmol), carbon tetrabromide (0.65 g, 1.95 mmol), and triphenylphosphine (0.54 g, 2.05 mmol) in methylene chloride (5 mL) was carried out as described for the preparation of MOPCH$_2$OC8Br to obtain MOPCH$_2$OC10Br (0.43 g, 95%) as white solid: mp 54-56 °C. ^{1}H-NMR (400 MHz, $CDCl_3$) δ 1.20-1.39 (m, 12H), 1.56 (q, 2H), 1.80 (q, 2H), 3.37 (t, 2H, J = 6.8 Hz), 3.46 (t, 2H, J = 6.5 Hz), 4.26 (s, 3H), 4.83 (s, 2H), 6.38 (d, 1H, J = 9.9 Hz), 6.92 (d, 1H, J = 2.2 Hz), 7.67 (d, 1H, J = 2.2 Hz), 8.13 (s, 1H, J = 9.9 Hz); ^{13}C-NMR (100 MHz, $CDCl_3$) δ 26.11, 28.09, 28.66, 29.29, 29.37, 29.46, 29.65, 32.76, 33.94, 61.32, 66.46, 70.73, 105.44, 114.57, 115.30, 120.74, 126.49, 132.58, 141.15, 143.79, 146.46, 146.98, 160.13; IR (cm^{-1}) 3116, 2932, 2851, 1733, 1587, 1461, 1427, 1379, 1311, 1132, 1093, 1038, 831, 753; Mass (m/e) 186, 201, 217, 229, 464; HRMS Calcd for $C_{23}H_{29}BrO_5$: 464.1198, found: 464.1273.

Preparation of MOPCH$_2$OC8Ad (11). MOPCH$_2$OC8Br (0.30 g, 0.69 mmol) was added to a stirred mixture of adenine (0.11 g, 0.82 mmol), K_2CO_3 (0.23 g, 1.65 mmol), and catalytic amounts of KI (10.0 mg) in DMF (10 mL). The stirring was continued for 72 hr at room temperature. The mixture was filtered and the filter cake was washed with ethyl acetate. Following removal of the solvent *in vacuo*, the residue was chromatographed with 10% methanol/methylene chloride to give MOPCH$_2$OC8Ad **11** (0.24 g, 71%) as a white solid: mp 139.5-140.2 °C. ^{1}H-NMR (400 MHz, $CDCl_3$) δ 1.22-1.26 (m, 8H), 1.49-1.54 (q, 2H), 1.82-1.85 (q, 2H), 3.43 (t, 2H, J = 6.5 Hz), 4.14 (t, 2H, J = 7.2 Hz), 4.24 (s, 3H), 4.81 (s, 2H), 5.83 (bs, 2H), 6.38 (d, 1H, J = 9.9 Hz), 6.90 (d, 1H, J = 2.2 Hz), 7.66 (d, 1H, J = 2.2 Hz), 7.62 (s, 1H), 8.11 (d, 1H, J = 9.9 Hz), 8.32 (s, 1H); ^{13}C-NMR (100 MHz, $CDCl_3$) δ 26.00, 26.52, 28.92, 29.10, 29.58, 30.00, 43.89, 61.33, 66.46, 70.58, 105.41, 114.58, 115.29, 119.65, 120.65, 126.52, 132.58, 140.51, 141.17, 143.74, 146.51, 146.93, 150.08, 152.60, 155.29, 160.17; IR (cm^{-1}) 3328, 3167, 3113, 2932, 2858, 1729, 1649, 1595, 1481, 1420, 1313, 1132, 1091, 1038, 917, 829, 729; Mass (m/e) 135, 149, 162, 176, 190, 204, 218, 229, 247, 261, 476, 491; HRMS Calcd for $C_{26}H_{29}N_5O_5$: 491.2168, found: 491.2160.

Preparation of MOPCH$_2$OC10Ad (12). Reaction of MOPCH$_2$OC10Br (0.43 g, 0.91 mmol), adenine (0.15 g, 1.10 mmol), K_2CO_3 (0.30 g, 2.20 mmol), and catalytic amounts of KI (15.0 mg) in DMF (9 mL) was carried out as described for the preparation of MOPCH$_2$OC8Ad to yield MOPCH$_2$OC10Ad **12** (0.25 g, 53%) as a white solid: mp 76.5-79 °C. ^{1}H-NMR (400 MHz, $CDCl_3$) δ 1.18-1.27 (m, 12H), 1.50-1.55 (q, 2H), 1.99-2.01 (q, 2H), 3.44 (t, 2H, J = 6.5 Hz), 4.15 (t, 2H, J = 7.2 Hz), 4.24 (s, 3H), 4.82 (s, 2H), 5.86 (bs, 2H), 6.38 (t, 2H, J = 9.9 Hz), 6.91 (d, 1H, J = 2.2 Hz), 7.66 (d, 1H, J = 2.2 Hz), 7.78 (s, 1H), 8.13 (d, 1H, J = 9.9 Hz), 8.32 (s, 1H); ^{13}C-NMR (100 MHz, $CDCl_3$) δ 26.09, 26.58, 28.94, 29.23, 29.27, 29.34, 29.64, 30.01, 43.94, 61.33, 66.46, 70.67, 105.42, 114.56, 115.31, 120.73, 126.52, 132.58, 140.54, 141.21, 143.77, 146.48, 146.96, 150.30, 152.58, 155.27, 157.69, 160.18; IR (cm^{-1}) 3328, 3167, 3113, 2932, 2858, 1729, 1649, 1595, 1481, 1420, 1313, 1132, 1091, 1038, 917, 829, 749; Mass (m/e) 135, 149, 162, 176, 190, 204, 229, 246, 275, 290, 504, 519; HRMS Calcd for $C_{28}H_{33}N_5O_5$: 519.2481, found: 519.2601.

Results and Discussion

UV absorption spectra. UV absorption spectra of MOPCH$_2$OCnAd show nearly the same pattern as the sum of UV spectra of MOPCH$_2$OC3 (219, 248, and 305 nm) and adenine (205 and 261 nm) in the range of 200-400 nm with the maximum intensities at 206 (ε = 35000 $M^{-1}cm^{-1}$), 255 (ε = 26000 $M^{-1}cm^{-1}$), 309 (ε = 10000 $M^{-1}cm^{-1}$), and a broad shoulder in the long UVA region of 310-380 nm in 5% ethanol/water as shown in Figure 2 and Table 1 and 2. The most striking feature characterizing the relationships between MOPCH$_2$OCnAd and 8-MOP is that absorption maximum of MOPCH$_2$OCnAd having two aromatic moieties tends to move toward longer wavelengths than 8-MOP and the fine structure tends to be decreased or broadened due to the increased intramolecular π-π stacking interaction in the folded conformation.[19] MOPCH$_2$OCnAd shows similar UV absorption as 8-MOPCH$_2$OC3 in the range of 310-380 nm.

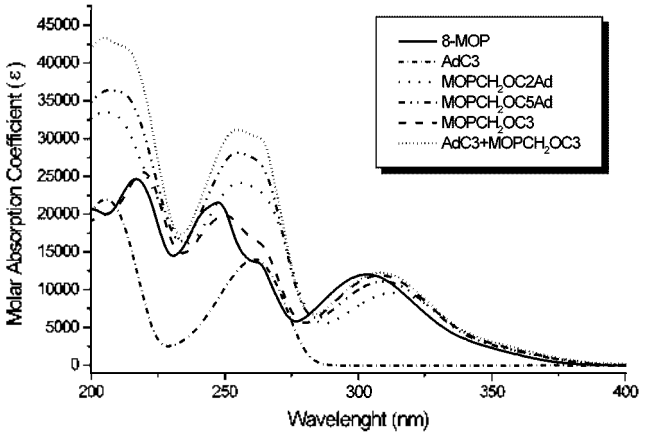

Figure 2. Ultraviolet absorption spectra of $MOPCH_2OCnAd$ (**7** and **9**, n = 2 and 5), AdC3, $MOPCH_2OC3$, 8-MOP (**1**), and AdC3+$MOPCH_2OC3$. All the spectra were measured under the same conditions: 5×10^{-5} M, 20 °C, 5% ethanol in water.

Table 1. UV absorption of $MOPCH_2OCnAd$ (n = 2, 3, 5, 6, 8 and 10) derivatives and 8-MOP (**1**) in 5% ethanol/water

Compound	λ_{max} (nm)	$\varepsilon \times 10^3$ ($M^{-1}cm^{-1}$)
8-MOP (**1**)	303.5	11.9
$MOPCH_2Ad$ (**6**)	–	–
$MOPCH_2OC2Ad$ (**7**)	313.4	9.6
$MOPCH_2OC3Ad$ (**8**)	310.8	10.9
$MOPCH_2OC5Ad$ (**9**)	309.2	11.1
$MOPCH_2OC6Ad$ (**10**)	308.6	11.5
$MOPCH_2OC10Ad$ (**12**)	–	–

Table 2. The absorption maximum (λ^a_{max}) of $MOPCH_2OC5Ad$ (**9**) in various solvents

Solvent	λ_{max} (nm)[a]	
Benzene	(–)[b]	302.2
Chloroform	(–)[b]	306.8
THF	(–)[b]	301.8
Methylene chloride	254.2	306.4
Acetonitrile	252.6	303.2
Ethanol	252.2	305.8
Methanol	253.2	305.4
5% Ethanol/water	255.0	309.2

[a]Measured at the concentration of 0.05 mM. The maximum absorbance was kept lower than 0.5. [b]Under the absorption window of solvents.

at which psoralen + UVA (PUVA) therapy is conducted.

In polar protic solvents, the absorption bands around 252 and 255 nm red shifted with increasing solvent polarity, showing that $\pi \rightarrow \pi^*$ transition is responsible for the absorption bands. The UVB absorption around 300 nm also showed a similar trend (λ_{max} of UVB absorption band red shifted from 302 nm in benzene to about 309 nm in 5% ethanol/water).

Fluorescence excitation and emission spectra. The fluorescence excitation and emission spectra of $MOPCH_2OCnAd$, $MOPCH_2OC3$, and 8-MOP in 5% ethanol/water

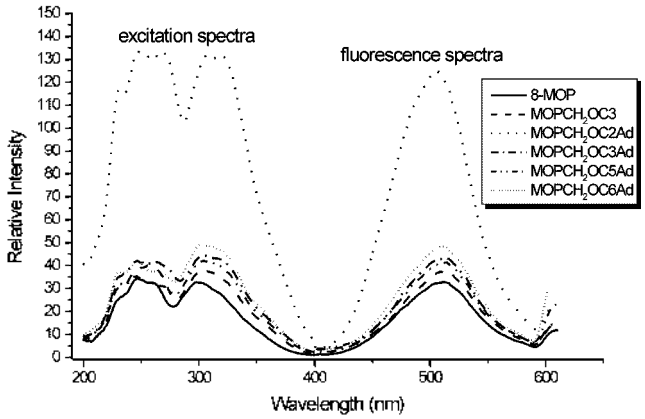

Figure 3. Fluorescence excitation (left) and emission (right) spectra of $MOPCH_2OC2Ad$ (**7**), $MOPCH_2OC3Ad$ (**8**), $MOPCH_2OC5Ad$ (**9**), $MOPCH_2OC6Ad$ (**10**), and 8-MOP (**1**), $MOPCH_2OC3$ in 5% ethanol/water at room temperature (excitation at 300 nm). Concentration was 2.5×10^{-5} M for all the solutions.

at room temperature are shown in Figure 3. The intensity of both excitation and emission spectra of $MOPCH_2OCnAd$ (n = 3, 5, 8), $MOPCH_2OC3$ and 8-MOP is much weaker than that of $MOPCH_2OC2Ad$. Two aromatic units linked by flexible polymethylene bridge can adopt folded and unfolded conformations in solution and the position of the folded ⟷ unfolded conformational equilibrium is a measure of the intramolecular ring-ring stacking interaction as reported earlier.[19] The model $MOPCH_2OC2Ad$ (**7**) in aqueous solvent is mostly in unfolded conformation stabilized through favorable solvation and H-bonding and consequently nonradiative decay paths like internal conversion or intersystem crossing are slowed down leading to strong fluorescence.

$MOPCH_2OC5Ad$ (**9**) is more flexible than $MOPCH_2OC2Ad$ (**7**) and can have strong π-π stacking interaction. $MOPCH_2OC5Ad$ (**9**), therefore, is chosen as a standard to investigate the solvent effects, H-bonding and solvation in particular, on the equilibrium of folded ⟷ unfolded conformation and π-π stacking interaction. Fluorescence emission spectra of $MOPCH_2OC5Ad$ (**9**) in various solvents at room temperature were recorded with λ_{ex} at 300 nm. The λ^f_{max} is shifted from

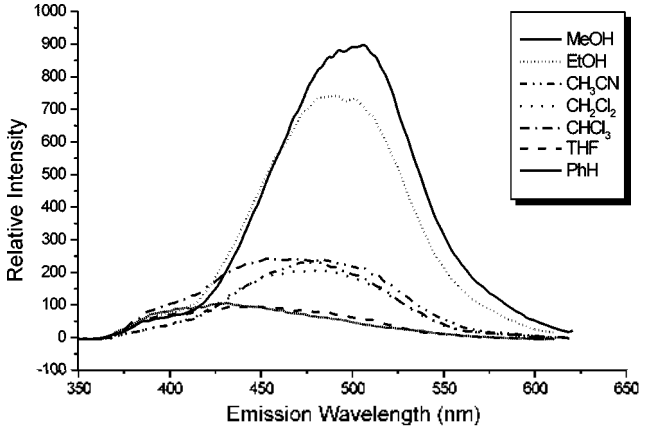

Figure 4. Fluorescence spectra of $MOPCH_2OC5Ad$ (**9**) in various solvents (excitation at 300 nm).

Table 3. Fluorescence intensity of $MOPCH_2OC5Ad$ (**9**) in various solvents at room temperature

Solvent	λ_{max}	Relative fluorescence intensity
Benzene	431.0	106
THF	447.5	96
Chloroform	471.0	240
Methylene chloride	478.5	206
Acetonitrile	482.5	240
Ethanol	490.5	741
Methanol	505.5	897

431 nm in benzene to 506 nm in methanol as shown in Figure 4 and Table 3. The λ^1_{max} showed bigger red shift with the increasing solvent polarity also indicating that fluorescent state is a ($\pi \rightarrow \pi^*$) state. The fluorescent intensity is enormously increased in protic polar solvents which favor unfolded conformation through H-bonding and polar solvation. The unfolded conformer becomes very rigid because of strong H-bonding and tight solvation and shows strong fluorescence. The fluorescence emission spectra in aprotic nonpolar solvents, in contrast, are broad and structureless due to the strong hydrophobic π-π stacking interaction between two aromatic units of the molecule in folded conformation, which leads to the formation of weakly or non-fluorescent excimer formation. The solvation of unfolded conformer is poor in nonpolar aprotic solvents because of ineffective H-bonding and weak polar interactions and folded conformer is dominant due to the strong hydrophobic interaction between two aromatic units of the molecule in nonpolar solvents.

Time-resolved fluorescence emission decay. The steady-state fluorescence in polar solvent is in sharp contrast to the behavior of nonpolar solvents as shown in Figure 4. Lim *et al*. demonstrated that the photophysical properties of the psoralens are strongly influenced by $S_1 \sim\!\!\rightarrow S_0$ internal conversion, the rate of which is highly dependent upon the solvent polarity, solvent viscosity, and temperature.[22] The

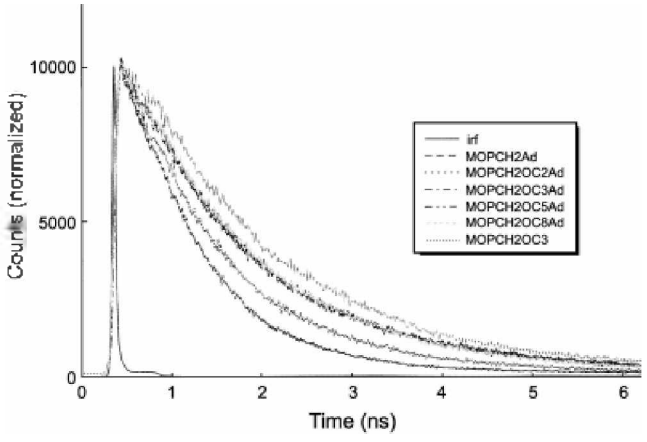

Figure 5. Time-resolved fluorescence decay curves of $MOPCH_2Ad$ (**6**), $MOPCH_2OCnAd$ (n = 2, 3, 5, and 8), and $MOPCH_2OC3$ (excitation at 293 nm).

Table 4. Fluorescence lifetime of $MOPCH_2Ad$ (**6**), $MOPCH_2OCnAd$, and $MOPCH_2OC3$[a]

Model and reference compounds	Short-lived component τ_1 (ps)	Long-lived component τ_2 (ps)	χ^2
$MOPCH_2Ad$ (**6**)	784 (97)[b]	4372 (03)	1.14
$MOPCH_2OC2Ad$ (**7**)	841 (73)	1850 (27)	1.18
$MOPCH_2OC3Ad$ (**8**)	709 (44)	1927 (56)	1.31
$MOPCH_2OC5Ad$ (**9**)	587 (28)	1672 (72)	1.17
$MOPCH_2OC8Ad$ (**11**)	600 (18)	1580 (82)	1.06
$MOPCH_2OC3$	475 (10)	1661 (90)	1.13

[a]Time-resolved fluorescence decay curves were obtained by TCSPC (time-correlated single photon counting) technique at the wavelengths of 293 and 520 nm for excitation and detection, respectively. Concentration was 5×10^{-5} M for all the solutions. Fluorescence lifetimes were estimated by exponential best fit. [b]Numbers in parentheses represent the contributions of each component, which is calculated from the pre-exponential factor.

dependence of the $S_1 \sim\!\!\rightarrow S_0$ internal conversion rate upon the solvent polarity can be rationalized in terms of the orientation of the polar solvent molecules in the reaction field of the electronically excited psoralens, which stabilize $S_1(\pi,\pi^*)$ relative to the higher lying $S_2(n,\pi^*)$ singlet state. The increased $S_1(\pi,\pi^*)$-$S_2(n,\pi^*)$ electronic energy gap resulting from this solvent reorientation (or relaxation) leads to a reduced proximity effect, and hence to a diminished $S_1 \sim\!\!\rightarrow S_0$ internal conversion rate.

Since the intensity of the fluorescence is very strong in protic polar solvents as shown in Figure 4, the fluorescence lifetime of $MOPCH_2OCnAd$ and $MOPCH_2OC3$ was measured by the TCSPC method in 5% ethanol/water. The fluorescence decay monitored at 520 nm consists of two decay components as shown in Figure 5. Fluorescence lifetime and calculated pre-exponential factor contributions (proportional to fluorescence intensities) are shown in Table 4. The fluorescent lifetimes of $MOPCH_2OCnAd$ in 5% ethanol/water solvent are 0.6-0.8 and 1.6-1.9 ns and those of $MOPCH_2OC3$ are 0.5 and 1.7 ns. It is noteworthy that the lifetime of the first component (about 0.7 ns) is shorter than that of the long-lived component (about 1.8 ns) at room temperature. Thus, the origin of this component should be different from that of the long-lived component at room temperature. This difference of the dual fluorescence decay in the polar protic solvent indicated that other species might be formed from the solvent reorientation(or relaxation). The long-lived component of fluorescence can be attributed to the relaxed species (*i.e.*, the species for which the solvent reorientation has occurred), while the short-lived components can be associated with the unrelaxed, or only partially relaxed, species. The rise time of the longer wavelength fluorescence is consistent with the solvent reorientation, which competes with the decay processes of the $S_1(\pi,\pi^*)$ state.

Conclusions

The fluorescence showed two exponential decay curves.

The long-lived component of fluorescence can be attributed to the relaxed species (*i.e.*, the species for which the solvent reorientation has occurred), while the short-lived components can be associated with the unrelaxed, or only partially relaxed, species. $MOPCH_2OCnAd$ shows similar UVA absorption spectra like $MOPCH_2OC3$ and 8-MOP. The λ^f_{max} showed the red shift with the increasing solvent polarity also indicating that fluorescent state is the $^1(\pi,\pi^*)$ state. Solvent effects on the red shift of UV absorption and fluorescence emission spectra indicate that the lowest excited singlet state is a $^1(\pi,\pi^*)$ state. The fluorescence emission spectra of $MOPCH_2OC5Ad$ in aprotic solvents were broad and structureless due to the excimer formation through the folded conformation. The intensity of fluorescence is dependent on the length of the bridging chain and $MOPCH_2OC2Ad$ shows the strongest fluorescence because the nonradiative decay paths like internal conversion or intersystem crossing are slowed down due to the unfolded conformation, which is strongly H-bonded and tightly solvated, particularly in protic polar solvents.

Acknowledgments. This work was supported by Korea Research Foundation Grant (KRF-2000-003-D00092).

References

1. (a) Song, P.-S.; Tapley, K. J. *Photochem. Photobiol.* **1979**, *29*, 1177. (b) Shim, S. C.; Jeon, Y. H.; Kim, D. W.; Han G. S.; Yoo, D. J. *J. Photosci.* **1995**, *2*, 37. (c) Shim, S. C. *Organic Photochemistry and Photobiology, CRC Handbook*; Horspool, W. M.; Song, P.-S., Eds.; CRC Press, Inc.: London, 1995; p 1347. (d) Zarebska, Z.; Waszkowska, E.; Caffieri, S.; Dall'Acqua, F. *Il Farmaco* **2000**, *55*, 515.
2. Scott, B. R.; Pathak, M. A.; Mohn, G. R. *Mutat. Res.* **1976**, *39*, 29.
3. (a) Parrish, J. A.; Stern, P. S.; Pathak, M. A.; Fitzpatrick, T. B. *The Science of Photomedicine*; Plenum Press: New York, 1982; pp 595-624. (b) Parrish, J. A.; Fitzpatrick, T. B.; Tanenbaum, L.; Pathak, M. A. *New Engl. J. Med.* **1974**, 1207.
4. Edelson, R.; Berger, C.; Gasparro, F.; Jegasothy, B.; Heald, P.; Wintroub, B.; Vonderheid, E.; Knobler, R.; Wolff, K.; Plewig, G.; Mekieman, G.; Christansen, I.; Oster, M.; Honigsmann, H.; Wilford, H.; Kokoschka, E.; Rehle, T.; Perez, M.; Stingl, G.; Laroche, L. *New Engl. J. Med.* **1987**, *316*, 297.
5. Knobler, R. M.; Honigsmann, H.; Edelson, R. L. Psoralen Phototherapies in *Psoralen DNA Photobiology*; Gasparro, F. T., Ed.; CRC Press: Boca Raton, Florida, 1988; Vol. II, pp 117-134.
6. Gorin, J.; Lessana-Leibowitch, M.; Fortier, P.; Leibowitch, J.; Escande, J.-P. *J. Am. Acad. Dermatol.* **1989**, *20*, 511.
7. Cimino, G. P.; Gamper, H. B.; Isaacs, S. T.; Hearst, J. E. *Annu. Rev. Biochem.* **1985**, *54*, 1151.
8. Hanson, C. V.; Shen, C.-K. J.; Hearst, J. E. *Science* **1976**, *193*, 62.
9. (a) Bordin, F.; Marzano, C.; Gatto, C.; Carassare, F.; Rodighiero, P.; Baccichetti, F. *J. Photochem. Photobiol. B: Biol.* **1994**, *26*, 197. (b) Chen, X.; Kagan, J.; DallAcqua, F.; Averbeck, D.; Bisagni, E. *J. Photochem. Photobiol. B: Biol.* **1994**, *22*, 51. (c) Fujita, H.; Sano, M.; Suzuki, K. *Photochem. Photobiol.* **1979**, *29*, 71.
10. Musajo, L.; Bordin, F.; Caporale, G.; Marciani, S.; Rigatti, G. *Photochem. Photobiol.* **1967**, *6*, 711.
11. (a) Rodighiero, G.; DallAcqua, F. *Photochem. Photobiol.* **1976**, 24, 647. (b) Parsons, B. J. *Photochem. Photobiol.* **1980**, *32*, 813.
12. DallAcqua, F.; Terbojevich, M.; Marciani Magno, S.; Vedaldi, D.; Recher, M. *Chem. Biol. Interact.* **1978**, *21*, 103.
13. Ronto, G.; Toth, K.; Gaspar, S.; Csik, G. *J. Photochem. Photobiol., B: Biol.* **1992**, *12*, 9.
14. Hearst, J. E.; Isaacs, S. T.; Kanne, D.; Rapoport, H.; Straub, K. *Q. Rev. Biophys.* **1984**, *17*, 1.
15. (a) Decout, J. L.; Huart, G.; Lhomme, J. *Photochem. Photobiol.* **1988**, *48*, 583. (b) Decout, J. L.; Lhomme, J. *Photochem. Photobiol.* **1983**, *37*, 155. (c) Decout, J. L.; Lhomme, J. *Tetrahedron Lett.* **1981**, *22*, 1247.
16. Castellan, A.; Desvergne, J. P. *Photochem. Photobiol.* **1981**, *34*, 183.
17. Kang, H. K.; Shin, H. J.; Shim, S. C. *J. Photochem. Photobiol. B: Biol.* **1992**, *13*, 19.
18. Yun, M. H.; Choi, S. J.; Shim, S. C. *Photochem. Photobiol.* **1993**, *58*, 164.
19. Yoo, D. J.; Hyun, S.-H.; Shim, S. C. *Bull. Korean Chem. Soc.* **2001**, *22*, 575.
20. Perrin, D. D.; Armarego, W. L. F. *Purification of Laboratory Chemicals*; Pergamon Press: New York, 1988.
21. Aboulezz, A. F.; El-Attar, A. A.; El-Sockary, M. A. *Acta Chim. Acad. Sci. Hung.* **1973**, *77*, 205.
22. Lai, T.-T.; Lim, B. T.; Lim, E. C. *J. Am. Chem. Soc.* **1982**, *104*, 7631.